(28)

# Remote sensing of global wetland dynamics with multiple satellite data sets

Catherine Prigent [1]
Département de Radioastronomie Millimétrique, Observatoire de Paris, Paris, France

Elaine Matthews, Filipe Aires, William B. Rossow
NASA/ Goddard Institute for Space Studies, New York, USA

Short title: SATELLITE REMOTE SENSING OF GLOBAL WETLANDS

Geophys. Res. Lett

**Abstract.** This study is the first global effort to quantify seasonality and extent of inundation with a suite of satellite observations, including passive and active microwave along with visible and infrared measurements. A clustering technique which merges the satellite observations is used to detect inundation. Monthly flooded areas are then calculated by estimating pixel fractional coverage of flooding using the passive microwave signal and a linear mixture model with end-members calibrated with radar observations to account for vegetation cover. The global results, comprising natural wetlands, irrigated rice, and lakes/rivers, indicate a minimum inundated area for the July 1992-June 1993 period of $2.16 \times 10^6 km^2$, about 38% of the maximum $5.75 \times 10^6 km^2$, to be compared to maximum areas of $5.83 \times 10^6 km^2$ and $5.7 \times 10^6 km^2$ from independent data sets. Comprehensive evaluation requires substantial additions to the sparse observational record now available.

## Introduction

Natural wetlands cover only ~4% of the Earth's ice-free land surface and rice paddies 1%. However, natural wetlands are the world's largest methane (CH4) source and the only one dominated by climate; with rice fields, wetlands account for ~40% of CH4 emitted annually to the atmosphere. While research now focuses on characterizing climate-driven variations in CH4 emissions [*Walter et al.*, 2001], one of the largest uncertainties in the global methane budget remains seasonal and interannual variations in wetland areas. Characterizing global wetland and dynamics is extremely difficult because they comprise a broad range of environments. Existing global data sets of natural wetlands and rice cultivation [e.g., *Matthews et al.*, 1987, 1991; *Cogley*, 1991] represent wetland distributions based essentially on vegetation and soils and rely on non-comparable wetland definitions. Remote sensing (RS) techniques employing visible, infrared and microwave observations offer varying degrees of success in quantifying wetland dynamics. *Sahagian and Melack*'s [1996] review concludes that the advantage of high spatial resolution of optical and infrared instruments is offset by their inability to penetrate clouds and vegetation making them inappropriate for global studies, although they can be useful in semi-arid environments [e. g. *Gumbricht et al.*, 2001]. Synthetic aperture radar (SAR) studies [e. g. *Hess et al.*, 1995] in the Amazon basin encompass large tropical forests with high spatial resolution (~100m) but large data volume limits the studies to a few mosaics preventing systematic, long-term assessments of inundation dynamics. Passive microwave observations are valuable for detecting flooded areas [e. g. *Gidding et al.*, 1989; *Sippel et al.*, 1998]. However, subsequent quantitative estimates of subpixel inundation extent are difficult using only passive microwave particularly when the flooded area is vegetated. Despite the recognized importance of wetlands in climate and biogeochemical cycles, and the large volume of satellite observations available, satellite techniques have not been systematically and globally investigated to assess their potential to detect inundated wetlands and to quantify their seasonal and spatial dynamics. The objective of this study is to demonstrate a globally applicable RS technique for detecting the dynamics of inundated areas of natural and anthropogenic wetlands using a suite of complementary satellite measurements.

## Data and Methodology

Satellite data with global coverage and multiple observations per month are selected for their potential to characterize inundated wetlands. An initial evaluation of the suitable observations performed by *Prigent et al.* [2001] provides a full description of these data sets. The selected observations cover a broad wavelength range: 1) passive microwave SSM/I emissivitis at 37 GHz; 2) ERS-1 active microwave scatterometer response at 5.25 GHz; 3) AVHRR Normalized Difference Vegetation Index (NDVI) derived from visible and near-infrared observations. Detection of inundation primarily relies on the passive microwave land-surface emissivities, estimated from SSM/I observations after removing contributions from the atmosphere, clouds, and rain [*Prigent et al.*, 1997]. Because the ERS scatterometer shows minimal response to the presence of inundation but is very sensitive to vegetation density [*Prigent et al.*, 2001], it is used to assess vegetation contributions to the passive microwave signal. In semi-arid regions where bare surfaces and inundations can produce similar passive microwave signatures, NDVI information is necessary to resolve ambiguities. All RS data for July 1992-June 1993 are composited/averaged monthly at an equal area resolution of 0.25° at the equator. Fig. 1 illustrates instrument responses for every other month of the study period for the Amazon basin and the Okavango delta. Microwave emissivities $\epsilon$ decline and polarization differences ($\Delta\epsilon = \epsilon V - \epsilon H$) rise with increasing inundation in both regions. For the Amazon, ERS backscatter $\sigma$ is stable in time and space and neither $\sigma$ nor NDVI display structures related to flooding. In semi-arid Botswana, the Okavango delta shows marked seasonality in all observations. Both $\epsilon$ and $\Delta\epsilon$ react to flooding while $\sigma$ and NDVI increase in response not to the standing water but to vegetation growth in inundated areas. We conclude from these and other sites that wetland detection with SSM/I passive microwave is feasible but additional observations responsive to vegetation changes are required to estimate the extent of inundated areas better. A suite of methodologies is developed to detect inundation and estimate the subpixel coverage of inundation by quantifying the contribution of vegetation to the passive microwave signal. An unsupervised clustering technique previously used to merge the RS data sets showed promising results for characterizing large-scale features of vegetation

density and seasonality [*Prigent et al.*, 2001]; the technique is refined for inundation detection. Sensitivity analyses determined the optimal subset of observations for input to the clustering scheme and the cluster analysis is applied simultaneously to the full suite of 12 monthly global data sets resulting in a subset of clusters associated with inundation. Because the response to inundation of emissivity polarization difference $\Delta e$ is modulated by vegetation, a method that accounts for the contribution of vegetation to $\Delta e$ is needed to quantify flooded area. $\Delta e$ increases with inundation fraction but declines with increasing vegetation density, whereas the ERS backscattering $\sigma$ is not very sensitive to the presence of inundation and increases with vegetation density. Figure 2 shows this relationship for all inundated pixels for all months. A linear mixture model is created from the statistical relationship between $\Delta e$ and $\sigma$ by assuming for each vegetation density value (represented by $\sigma$) that $\Delta e$ varies linearly with subpixel inundation fraction. Two end-members for each vegetation density (each dB in $\sigma$) in the linear mixing model are determined by the mean for the lowest 10% of $\Delta e$ values, assumed to correspond to 5% inundation, and the meean of the highest 10% of the $\Delta e$ values, assumed to correspond to 95% inundation (open circles in Fig. 2). Because there is no tuning to individual wetlands or ecosystems, this mixture model is used to calculate flooded fractions for inundated pixels globally for all months of the study period.

## Results and Discussion

Assessment focuses on the large-scale distributions of inundation seasonality or duration, and areas. Since our method does not distinguish among standing water in natural wetlands, irrigated rice fields, and large lakes/rivers, we compare the new results (Fig. 3a,b) with multiple, independent data sets that together capture the full complement of potential inundation. These data sets do not necessarily reflect seasonal dynamics (Fig. 4). *Matthews and Fung*'s [1987] wetland fractions (Fig. 3c) come from aeronautical charts, the information for which is more likely acquired during warm seasons of maximum flooding. *Matthews et al.*'s [1991] monthly cultivated-rice areas (Fig. 3d) were derived from area statistics and seasonal cropping calendars making this data set directly comparable to maximum inundation from the new study. The wetland data set from *Cogley* [1991] includes irrigated rice for some regions

(China) and not others (India) (Fig. 3e). The lake data set (Fig. 3f) shows very broad distributions of small lakes in boreal regions of the western hemisphere.

The new results exhibit very realistic structures. Asian rice paddies have a strong signature, especially in India, and Bangladesh, where rice dominates agricultural landscapes (Fig. 3a): Inundation duration is consistent with the number and duration of rice crops [*Matthews et al.*, 1991]. In boreal regions, inundation periods decline from ~5 months around 45° to ~3 months around 55°, consistent with other observations. Major inundated wetlands are well delineated in all latitudes and environments (Fig. 3b). The Pantanal and riverine wetlands along the Amazon are clearly captured in South America. The Niger delta (Mali) and wetlands associated with lake Chad in semi-arid Africa are realistically represented. The inundated region around the Ob river in northern Russia is well reproduced. The extensive features in Canada are similar to *Cogley*'s lake data (Fig. 3f) but probably reflect short-duration complexes of pools and inundated tundra. In contrast, although inundation in central east Africa appears underestimated relative to other compilations, detailed analyses of satellite observations show no signatures indicating flooding, so further investigation is required.

Inundated area estimates depend on the validity of the mixture model which cannot be comprehensively calibrated due to the scarcity of observations to quantify responses of vegetation/inundation mixtures over representative wetlands. In addition, very few observations are available for wetland areas, particularly their seasonal variations, and there are no data sets reporting global dynamics of areas over a year or longer. In central Amazon (0S8S 72W54W), *Hess et al.* (personal communication) estimate a maximum inundated area of $3.0 \times 10^5 km^2$ from SAR, whereas *Matthews and Fung* predict a static value of $0.4 \times 10^5 km^2$ and *Cogley* $0.2 \times 10^5 km^2$ of wetland and $0.1 \times 10^5 km^2$ of lakes. Our method gives a maximum extent of $1.6 \times 10^5 km^2$. In the Okavango delta (21S18S 22E24E), maximum inundation extent (3,800 $km^2$) is close to estimates from both *Matthews and Fung* (4,660 $km^2$) and *Cogley* (3,970 $km^2$). Inundation seasonality agrees well with *Gumbricht et al.* [2001] based on NDVI data although the latter predict a maximum area of 16,000 $km^2$ which might be an overestimate since NDVI responds not to inundation per se but to vegetation associated with water and

therefore may include vegetation on the perimeter of standing water as well as vegetation growing after inundation.

Globally, the new results indicate a minimum inundated area of $2.16 \times 10^6 km^2$, about 38% of the maximum of $5.75 \times 10^6 km^2$, for the 12-month period; these areas comprise natural wetlands, rice fields and lakes/rivers. *Matthews and Fung* [1987] report a total natural wetland area of $5.30 \times 10^6 km^2$ of which about 60% or $3.18 \times 10^6 km^2$ is inundated during some part of the year; $1.2 \times 10^6 km^2$ of irrigated rice fields at maximum cultivation [*Matthews et al.*, 1991] gives a total maximum wetland inundation of $4.38 \times 10^6 km^2$. Adding Cogley's lake/river area ($1.45 \times 10^6 km^2$) gives $5.83 \times 10^6 km^2$. The *Cogley* data yield a similar wetland-plus-rice area of $4.25 \times 10^6 km^2$; the lake/river area adds to a total of $5.7 \times 10^6 km^2$. Each of these results are derived with completely different data and techniques. However, while the agreement is encouraging and provides some confidence in the new RS technique, it is important to note that the uncertainty in seasonal inundation dynamics is greater than these close values indicate because the similarities may result in part from fortuitous compensating differences among the data sets.

## Conclusion

This study reports the first effort to quantify seasonality and extent of global inundation with a clustering analysis of a suite of satellite observations covering a wide spectral range including passive and active microwaves, visible and near-IR observations, together with a linear mixing model to estimate inundated pixel fractions. The technique is globally applicable without any tuning for individual environments. Global inundated area varies from a $5.75 \times 10^6 km^2$ maximum to a $2.16 \times 10^6 km^2$ minimum for natural wetlands, irrigated rice fields and lakes/rivers, comparable to values obtained from independent data. At present, more conclusive assessment of distribution, inundation duration, and areas is hampered by the scarcity of quantitative observations, particularly seasonal and interannual, for many wetland complexes. With further validation, an approach based on global satellite observations could provide information on the interannual variations of inundation over more than a decade.

## References

Cogley, J.G., GGHYDRO-Global Hydrographic data release 2.0, Trent Climate note 91-1, Trent Univ., 12, 1991.

Giddings, L. and B.J. Choudhury, Observation of hydrological feature with Nimbus-7 37GHz data applied to South America, *Int. J. Remote Sens.*, *10*, 1673-1686, 1989.

Gumbricht, T., J. McCarthy, T. McCarthy, Portraying the geophysiology of the Okavango delta, Bostwana, submitted, 2001.

Hess, L., J.M. Melack, S. Filoso and Y. Wang, Delineation of inundated area and vegetation along the Amazon floodplain with the SIR-C Synthetic Aperture Radar, *IEEE Trans. on Geosci. Remote Sens.*, *33*, 896-903, 1995.

Matthews, E., and I. Fung, Methane emission from natural wetlands: global distribution, area, and environmental characteristics of sources, *Glob. Biogeochem. Cycles*, *1*, 61-86, 1987.

Matthews, E., I. Fung, and J. Lerner, Methane emission from rice cultivation: geographic and seasonal distribution of cultivated areas and emissions, *Glob. Biogeochem. Cycles*, *5*, 3-24, 1991.

Prigent C., W.B. Rossow, E. Matthews, Microwave land surface emissivities estimated from SSM/I observations, *J. Geophys. Res.*, *102*, 21867-21890, 1997.

Prigent, C., F. Aires, W.B. Rossow, E. Matthews, Joint characterization of vegetation by satellite observations from visible to microwave wavelength: A sensitivity analysis, *J. Geophys. Res.*, in press, 2001.

Sahagian, D., and J. Melack (Eds.) Global wetland distribution and functional characterization: Trace gases and the hydrologic cycle, Wetlands Workshop Report, IGBP workshop, Santa Barbara, CA, 1996.

Sippel, S.J., S.K. Hamilton, J. M. Melack, and E. M. Novo, Passive microwave observations of inundation area and area/stage relation in the Amazon river floodplain, *Int. J. Remote Sens.*, *19*, 3055-3074, 1998.

Walter, B., M. Heimann, E. Matthews, Modeling modern methane emissions from natural wetlands, 2. Interannual variations 1982-1993, *J. Geophys. Res.*, in press, 2001.

C. Prigent, Département de Radioastronomie Millimétrique, Observatoire de Paris, 61, Avenue de l'Observatoire, 75014 Paris, France. (e-mail: Catherine.Prigent@obspm.fr)

E. Matthews, F. Aires, and W. Rossow NASA/ Goddard Institute for Space Studies, 2880 Broadway, New York, NY 10025, USA. (e-mail: ematthews@giss.nasa.gov; wrossow@giss.nasa.gov; faires@giss.nasa.gov)

Received _____

[1]Previously at NASA/ Goddard Institute for Space Studies, New York, USA

**Figure 1.** Responses of the three instruments over wetlands, for every other month between July 1992 and June 1993: (a) the Amazon rainforest around Tabatinga in Brasil, (b) the Okavango delta in Botswana. For the passive microwaves, the 37 GHz emissivities are plotted for both polarizations and for their difference. The ERS-1 backscattering coefficient is presented. The AVHRR NDVI is presented at its 8 km resolution pathfinder resolution.

**Figure 2.** Scatterplot of the ERS scatterometer backscattering $\sigma$ versus the emissivity polarization difference at 37 GHz $\Delta e_{37}$ for all pixels that are classified as inundated. For each 1 dB range of $\sigma$, mean $\Delta e_{37}$ are calculated for the 10 % lowest and highest $\Delta e_{37}$. The resulting values are plotted on the graph.

**Figure 3.** a) Number of inundated months for each 0.25°x0.25° pixel for the globe for the July 1992-June 1993 period, whatever the fractional inundation within a pixel (satellite estimation); b) fractional inundation at the maximum over the year calculated on a 1° grid (satellite estimation); c) fractional extent of natural wetlands [*Matthews and Fung*, 1987]; d) fractional extent of rice cultivation at the maximum [*Matthews et al.*, 1991]; e) fractional extent of wetlands [*Cogley*, 1991]; f) fractional extent of lakes [*Cogley*, 1991].

**Figure 4.** Seasonal variations of the inundated areas globally and by latitude zones. Static estimates from *Matthews et al.* and *Cogley* are also indicated.

Color figures

Fig. 1

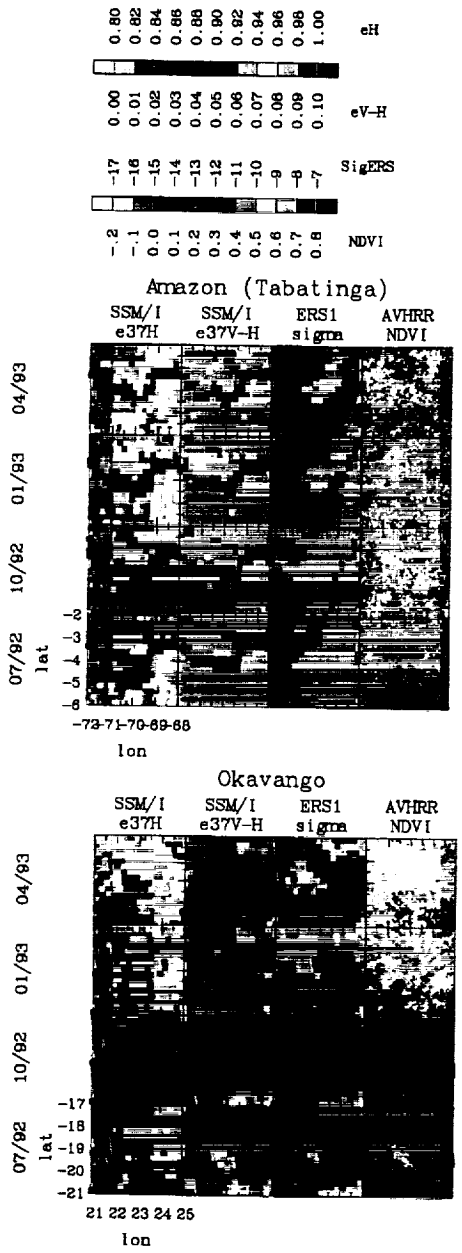


Fig. 3 a b c d e f

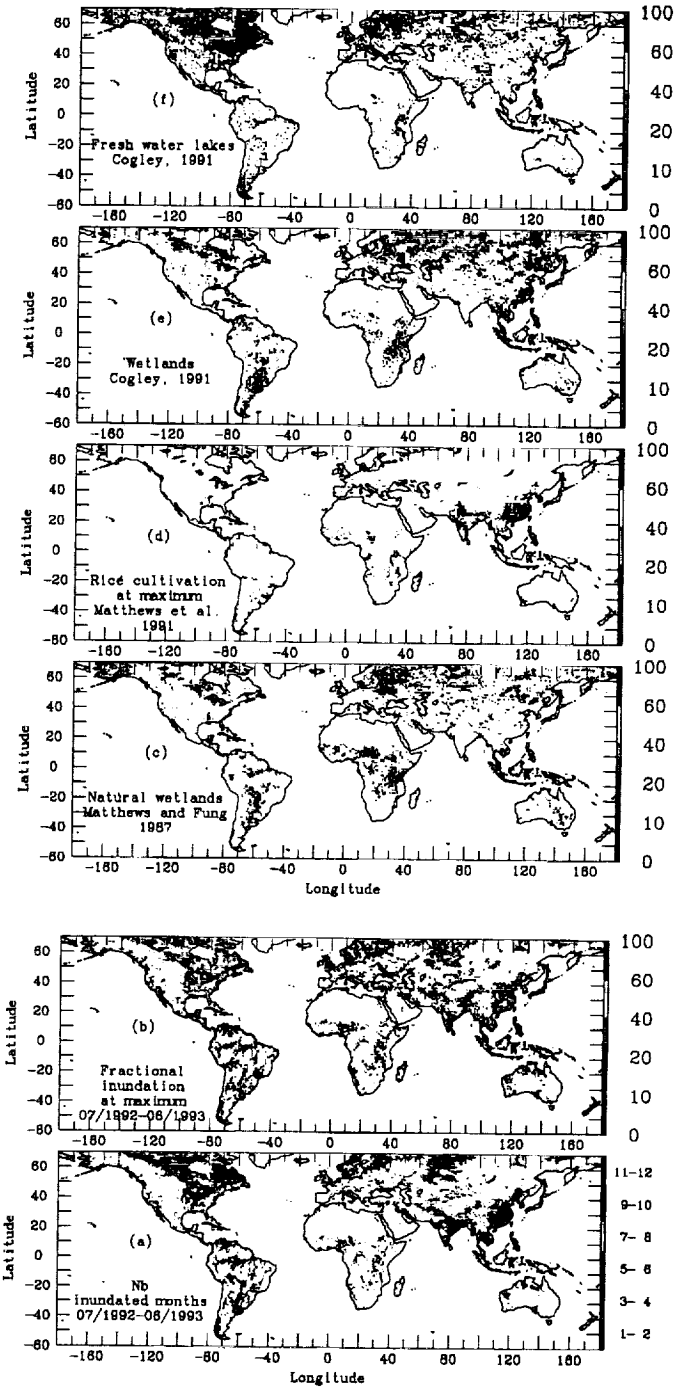

Fig. 2

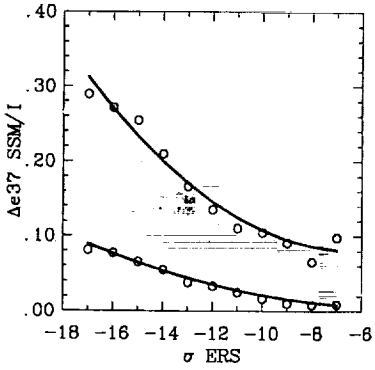
.40
.30
.20
.10
.00
Δe37 SSM/I
−18 −16 −14 −12 −10 −8 −6
σ ERS

Fig. 4

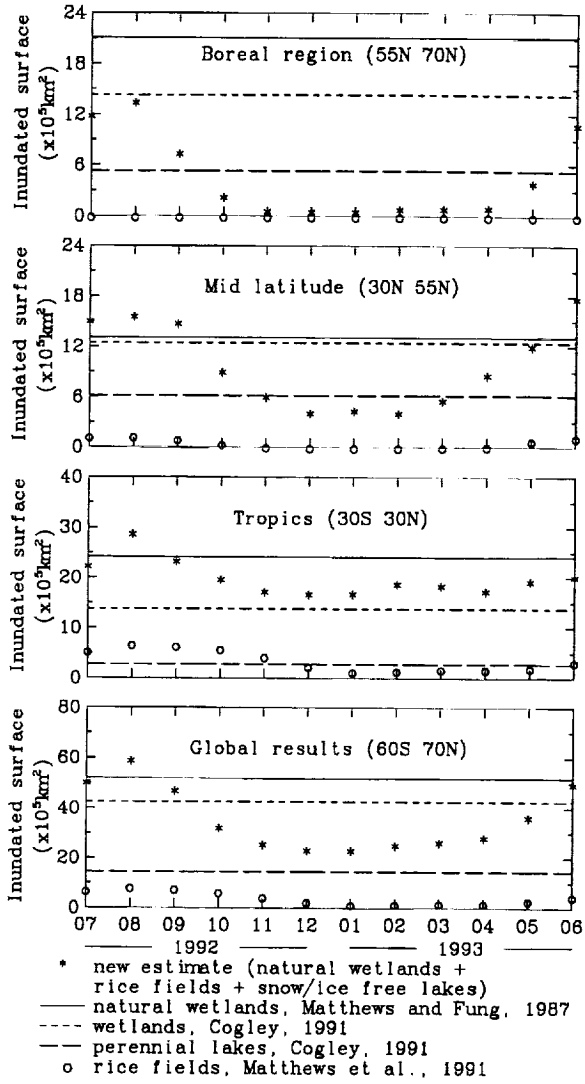
Boreal region (55N 70N)
Mid latitude (30N 55N)
Tropics (30S 30N)
Global results (60S 70N)
Inundated surface (x10⁵km²)
07 08 09 10 11 12 01 02 03 04 05 06
1992
1993
* new estimate (natural wetlands + rice fields + snow/ice free lakes)
natural wetlands, Matthews and Fung, 1987
wetlands, Cogley, 1991
perennial lakes, Cogley, 1991
o rice fields, Matthews et al., 1991